Research article

MRC

Received: 18 February 2015 Accepted: 28 April 2015 Published online in Wiley Online Library: 12 June 2015

(wileyonlinelibrary.com) DOI 10.1002/mrc.4265

Investigation of chloromethane complexes of cryptophane-A analogue with butoxy groups using ^{13}C NMR in the solid state and solution along with single crystal X-ray diffraction

Emilie Steiner,[a] Renny Mathew,[a] Iwan Zimmermann,[a] Thierry Brotin,[b] Mattias Edén[a] and Jozef Kowalewski[a]*

Host-guest complexes between cryptophane-A analogue with butoxy groups (cryptophane-But) and chloromethanes (chloroform, dichloromethane) were investigated in the solid state by means of magic-angle spinning ^{13}C NMR spectroscopy. The separated local fields method with ^{13}C-^{1}H dipolar recoupling was used to determine the residual dipolar coupling for the guest molecules encaged in the host cavity. In the case of chloroform guest, the residual dipolar interaction was estimated to be about 19 kHz, consistent with a strongly restricted mobility of the guest in the cavity, while no residual interaction was observed for encaged dichloromethane. In order to rationalize this unexpected result, we performed single crystal X-ray diffraction studies, which confirmed that both guest molecules indeed were present inside the cryptophane cavity, with a certain level of disorder. To improve the insight in the dynamics, we performed a ^{13}C NMR spin-lattice relaxation study for the dichloromethane guest in solution. The system was characterized by chemical exchange, which was slow on the chemical shift time scale but fast with respect to the relaxation rates. Despite these disadvantageous conditions, we demonstrated that the data could be analyzed and that the results were consistent with an isotropic reorientation of dichloromethane within the cryptophane cavity. ***Magnetic Resonance in Chemistry*** **published by John Wiley & Sons Ltd.**

Keywords: ^{13}C NMR; dipolar couplings; relaxation; X-ray diffraction

Introduction

Cryptophanes are cage-like compounds consisting of two equivalent cyclotribenzylene caps, often carrying substituents on the phenyl rings and connected by flexible –O-$(CH_2)_n$-O-linkers. The first cryptophane synthesized by Collet *et al.* in 1981[1,2] was an *anti*-isomer, carrying one methoxy group on each phenyl ring with three caps, often carrying ($n = 2$) linkers and was called cryptophane-A. Cryptophanes can act as molecular hosts, forming inclusion complexes with small organic molecules (such as chloromethanes),[3,4] as well as with xenon atoms.[5] The chemistry of cryptophanes has been reviewed a few years ago.[6] The cryptophane-A analogue with butoxy substituents instead of methoxy groups – called cryptophane-But – was prepared by Brotin *et al.*[7,8] The structure of cryptophane-But is shown in Fig. 1. We have recently reported a study of the chloromethane complexes of cryptophane-A and cryptophane-But using a variety of liquid-state NMR techniques.[9] Here, we extend this work by studying cryptophane-But complexes with dichloromethane and chloroform in the solid state, using ^{13}C NMR and single-crystal X-ray diffraction (XRD). We thereby exploit the fact that cryptophane-But is readily prepared in the crystalline form. Solid cryptophane complexes with chloromethane guests have previously been studied using XRD by the Collet group,[10,11] by our laboratory[12] and by Taratula and co-workers.[13] Solid-state investigations of chloromethane@cryptophane systems, using the deuteron NMR[12] and ^{13}C NMR[14] have also been reported.

In this paper, we report solid-state ^{13}C cross-polarization (CP) magic-angle spinning (MAS) NMR spectra for CH_2Cl_2 and $CHCl_3$ complexed by cryptophane-But, where two-dimensional MAS spectra obtained using the separated local fields (SLF) method inform about the motionally averaged ^{13}C-^{1}H dipolar couplings.[15] Because the results turned out to deviate from our expectations, we also gained complementary information from single crystal XRD studies of both complexes, as well as ^{13}C NMR relaxation experiments in solution for CH_2Cl_2@cryptophane-But.

Experimental

Materials

Cryptophane-But was synthesized following the method of Brotin *et al.*[7,8] ^{13}C-labelled chloroform and dichloromethane, as well as

* *Correspondence to: Jozef Kowalewski, Department of Materials and Environmental Chemistry, Arrhenius Laboratory, Stockholm University, SE-106 91 Stockholm, Sweden. E-mail: jozef.kowalewski@mmk.su.se*

a *Department of Materials and Environmental Chemistry, Arrhenius Laboratory, Stockholm University, SE-106 91, Stockholm, Sweden*

b *Laboratoire de Chimie, (CNRS-UMR 5182) Ecole Normale Supérieure de Lyon, 46 Allée d' Italie, F-69364, Lyon Cedex 07, France*

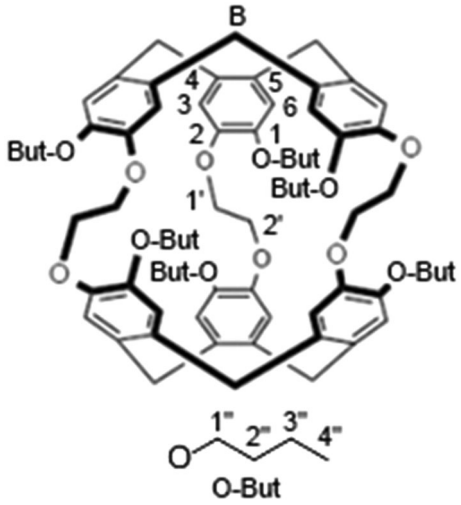

Figure 1. Schematic structure of cryptophane-But.

the deuterated solvent, 1,1,2,2-tetrachloroethane-d_2, were obtained from Cambridge Isotope Laboratory, while non-labelled chloroform and dichloromethane were purchased from Sigma-Aldrich (St. Louis, Mo, USA).

Sample preparations and methods

Solid-state NMR

For the solid-state NMR experiments, two powder samples were prepared by dissolving cryptophane-But in a mixture containing a 1 :10 ratio of ^{13}C-labelled and natural abundance chloroform or dichloromethane. The two mixtures were left to evaporate at room temperature over 2 days. The crystals obtained were then ground and packed in 4 mm zirconia pencil rotors that were spun at a 9.00 kHz MAS frequency throughout all NMR experiments.

The solid-state experiments were performed at 9.4 T (−400.07 MHz ^{1}H Larmor frequency) using a Bruker Avance-III spectrometer (Rheinstetten, Baden-Württemberg, Germany). All experimentation on $CHCl_3$@cryptophane-But and CH_2Cl_2@cryptophane-But was carried out at temperatures of 268 and 238 K, respectively. In the case of CH_2Cl_2@cryptophane-But, additional experiments were also carried out at a lower temperature of 203 K (not shown); no significant differences were observed at the two temperatures. All NMR experimentation started with a ramped[16] CP pulse block, using ^{13}C and H nutation frequencies of 50 ± 5 and 59 kHz, respectively, contact intervals of 5.0 ms ($CHCl_3$@cryptophane-But) and 2.5 ms (CH_2Cl_2@cryptophane-But) and relaxation delays of 5 s throughout. The 90° proton pulse prior to CP operated at 83 kHz. High-power decoupling at 83 kHz using the two pulse phase modulation (TPPM) scheme[17] ($\tau_p = 5.8\,\mu s$ and $\Delta\varphi = 15°$) was used during the NMR signal acquisitions in both 1D and 2D NMR measurements. Chemical shifts are referenced externally to neat tetramethylsilane.

The 2D SLF recoupling experiments utilized the constant-time protocol of ref. 18 and the symmetry-based $R18_1^7$ pulse sequence[18,19] for reintroducing the heteronuclear ^{13}C-^{1}H interactions. It is based on a repeating pair of 180° pulses, $180_{70}180_{-70}$ (where each subscript denotes the rf phase in degrees) that demands a ^{1}H nutation frequency of exactly 9 times the MAS rate,[18,19] i.e. 81 kHz for the present experimentation. The 2D NMR acquisitions involved 4994 t_2 increments and 40 ($CHCl_3$@cryptophane-But) and 80 (CH_2Cl_2@cryptophane-But) t_1-increments, with the respective dwell times $\Delta t_2 = 20.0\,\mu s$ and $\Delta t_1 = 37.04\,\mu s$ (the latter implying that t_1 was sampled after completion of six 180^0-pulse pairs of the repeating $R18_1^7$ scheme); this provided spectral windows of 50 and 27 kHz along the direct and indirect spectral dimensions, respectively. The 2D data sets were zero-filled to $512(t_1) \times 8192(t_2)$ time points and apodized by 250 Hz Gaussian (t_1) and 20 Hz Lorentzian (t_2) full width at half maximum broadening before 2DFT of the s(t_1, t_2) data set. A cosine Fourier transform was used in the indirect dimension. The ^{1}H rf carrier frequency was set at the middle of the proton spectrum (5 ppm), while that of ^{13}C was at 77 and 51 ppm for $CHCl_3$ and CH_2Cl_2, respectively. The 180° ^{13}C pulse for chemical shift-refocussing that appears at the centre of the constant time interval $T = 4.4$ ms operated at 90 kHz. The remaining of T not involving $R18_1^7$ pulsing decoupled the heteronuclear interactions by a CW field at 85 kHz (see ref. 18). The total number of scans per t_1 value was 40 for $CHCl_3$@cryptophane-But and 80 for CH_2Cl_2@cryptophane-But.

Numerically, exact simulations of the heteronuclear recoupling segment of the 2D SLF experiment on $CHCl_3$@cryptophane-But assumed an isolated ^{13}CH group in the presence of the $R18_1^7$ recoupling sequence. The calculations included all relevant experimental parameters (MAS rate, rf pulses and ^{13}C-^{1}H interaction) and employed 500 Hz full width at half maximum Lorentzian line broadening. All numerical procedures followed those outlined in detail in our previous work.[4]

X-ray diffraction

Crystals for the XRD measurements were obtained by dissolving the cryptophane-But in chloroform or dichloromethane at near-critical concentrations. The single crystals were obtained from a slow controlled solvent evaporation and, once selected, were directly covered with epoxy glue to prevent them from deterioration during the diffraction experiments.

Single crystal XRD experiments were performed on an Oxford Diffraction Xcalibur3 (Oxford Instruments, Oxford, UK) diffractometer equipped with a graphite monochromator. The data were collected at room temperature using Mo Kα radiation ($\lambda = 0.71073$ Å). Absorption correction and data reduction were performed with the software CrysAlis RED which was also employed for the analytical absorption correction.[20] The structure solution was carried out with SIR97[21] and the refinement with SHELXL[22] in the WinGX[23] environment.

Direct methods (SIR97) yielded reasonable atomic positions for the cryptophane. Severe structural disorder was found to be present in the butoxy groups. Thus, the C–C distances to the nearest and the next nearest neighbour were restricted to 1.54 and 2.52 Å, respectively, in order to obtain regular carbon chains having C–C–C bond angles close to 110°. The butoxy groups were found to occupy two almost equally populated positions. Minor disorder was also observed in the carbon atoms belonging to the linkers.

The atomic positions for the guest molecules were located in the difference Fourier map. Both dichloromethane and chloroform were disordered over several positions. The distances of the guest molecules were restrained (C-Cl: 1.7 Å) to obtain a reasonable molecular geometry. All occupancies for the disordered guest positions were refined to fully occupy the host cavity.

Hydrogen atom positions were generated in expected positions and refined using the default parameters in SHELXL. No hydrogen atoms were assigned to the guest molecules. Non-hydrogen atoms

were refined anisotropically, except for the carbon atom in the guest chloroform that was refined isotropically.

The crystal data and selected details of the reduction and refinement calculations are summarized in Table 1. The structures were drawn with the program DIAMOND.[24] The electron density maps were calculated in WinGX[23] and displayed in VESTA.[25]

Solution-state NMR

Cryptophane-But was dipped into non-labelled dichloromethane, and the solvent was then let to evaporate. This process was repeated three times to remove undesirable products that potentially formed during synthesis. For this work, a sample containing 11 mM cryptophane-But and 13 mM CH_2Cl_2 in 1,1,2,2-tetrachloroethane-d_2 was used. This sample corresponds to specimen number 4 in the earlier work from our laboratory.[9]

The liquid-state experiments were run on a Bruker Avance spectrometer operating at 14.1 T with a 5 mm TXI probehead. Temperature calibration (±1 K) was performed by using a resistance detector made of copper wire dipped into silicon oil contained in a 5 mm tube.

The spin-lattice relaxation time T_1 of dichloromethane@-cryptophane-But was measured by a series of 2D inversion-recovery ^{1}H-^{13}C HSQC experiments[26] using a double INEPT transfer[27] (with a delay equal to $1/4J_{CH} = 1.4$ ms for CH_2Cl_2) and sensitivity improvement.[28] The number of real data points acquired was 128 in the t_1 dimension (^{13}C) and 2048 in the t_2 dimension with a spectral width of 10 ppm in the ^{1}H dimension and 100 ppm in the ^{13}C dimension. Echo-antiecho acquisition[29] was used for frequency-sign discrimination in the ν_1 dimension. For these experiments, 32 scans and a recycle delay of 3 s were used. The T_1 determination was based on the acquisition of 12 spectra with inversion-recovery delays ranging from 5 ms to 3 s.

Data were processed with the Bruker Topspin software. Linear prediction was applied in the indirect dimension, followed by apodization with a squared-cosine-bell function.

Results and discussion

Solid-state NMR

Figure 2 shows the ^{13}C CPMAS spectra recorded from the (a) $CHCl_3$@cryptophane-But and (b) CH_2Cl_2@cryptophane-But samples, both revealing NMR signals from the guest molecules assuming encaged as well as interstitial positions. In an alternative

Table 1. Crystal data and structure refinement parameters

Empirical formula	$C_{72}H_{90}O_{12} \cdot CHCl_3$	$C_{72}H_{90}O_{12} \cdot CH_2Cl_2$
Formula weight (g/mol)	1265.80	1230.35
Temperature (K)	293	293
Wavelength (Å)	0.71073	0.71073
Crystal system	Trigonal	Trigonal
Space group	*R*-3*c* (No. 167)	*R*-3*c* (No. 167)
a (Å)	17.2579(9)	17.2060(7)
b (Å)	17.2579(9)	17.2060(7)
c (Å)	40.398(2)	40.4426(16)
α (°)	90	90
β (°)	90	90
γ (°)	120	120
Volume (Å^3)	10420.0(9)	10368.8(7)
Z	6	6
Density$_{calc.}$ (g cm^{-3})	1.210	1.183
Absorption coefficient (mm^{-1})	0.191	0.153
F(000)	4050	3948
Crystal colour	Colourless	Colourless
Crystal habit	Block	Block
Crystal size (mm^3)	0.188 × 0.169 × 0.088	0.445 × 0.288 × 0.169
Theta range for data collection (°)	3.39–28.82	3.40–27.72
Index ranges	$-23 \le h \le 10$ $-6 \le k \le 22$ $-54 \le l \le 50$	$-22 \le h \le 22$ $-21 \le k \le 21$ $-52 \le l \le 52$
Reflections collected / unique	7325/2686 ($R_{int} = 0.043$)	20569/2526 ($R_{int} = 0.040$)
Reflections [$I > 2$sigma(I)]	1284	1598
Data/restraints/parameters	1284/16/194	1598/19/208
Goodness-of-fit on F^2	0.998	1.170
Final *R* indices[a]	$R_1 = 0.0760$ $wR_2 = 0.1649$	$R_1 = 0.0793$ $wR_2 = 0.1658$
[$I > 2$sigma(I)]		
R indices (all data)	$R_1 = 0.1628$ $wR_2 = 0.2104$	$R_1 = 0.1309$ $wR_2 = 0.1867$
Largest diff. peak and hole (eÅ^{-3})	0.18 and −0.13	0.13 and −0.12

[a] $R_1 = \sum||F_o| - |F_c|| / \sum|F_o|$; $wR_2 = \{\sum[w(F_o^2 - F_c^2)^2] / \sum[w(F_o^2)^2]\}^{1/2}$

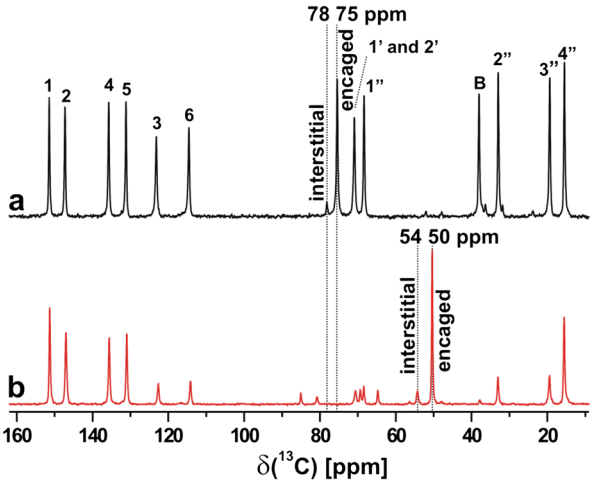

Figure 2. ^{13}C cross-polarization magic-angle spinning spectra recorded at 9.4 T and a magic-angle spinning frequency of 9.0 kHz from powders of (a) $CHCl_3$@cryptophane-But and (b) CH_2Cl_2@cryptophane-But at temperatures of 268 and 238 K, respectively. The resonances from 'interstitial' and 'encaged' guest molecules are marked; the remaining atom numbers correspond to those of Fig. 1.

interpretation, one could consider the 'interstitial' signal as arising from chloromethane adsorbed on the surface of the crystals. The ^{13}C chemical shifts of the encaged guests accord very well with those obtained by solution NMR (not shown). This observation is in agreement with our earlier work.[4,14]

Figure 3 displays the respective 2D SLF ^{13}C NMR spectra. Each CH_n moiety exhibiting a significant residual heteronuclear contact produces a 'split lineshape' along the horizontal spectral dimension, with the splitting reflecting the size of the recoupled dipolar ^{13}C-^{1}H interaction(s).[18] The 2D NMR spectrum from $CHCl_3$@cryptophane-But is shown in Fig. 3a (left panel), together with slices (right panel) revealing the recoupled ^{13}C NMR peak-shapes observed from the interstitial and encaged $CHCl_3$ molecules. While the former signal is narrow, that associated with the encaged molecules reveals the three-peak pattern expected from a ^{13}C-^{1}H moiety with a significant residual dipolar interaction.[19] The accompanying best-fit numerical simulation (red trace) reproduces well the experimental splitting of 5.46 kHz between the outer peaks when using a dipolar coupling constant of $|b_{C\text{-}H}| = 19.0$ kHz. The C–H bond length in chloroform is reported as 107.3 pm from the microwave spectrum,[30] which translates into a rigid dipolar coupling constant of 24.0 kHz. The ratio of 0.792 between the motionally averaged residual dipolar coupling and its rigid counterpart is equivalent with an order parameter for the encaged molecule, the square of which can be compared with the generalized order parameter squared from relaxation data in solution (see succeeding discussions). For interstitial chloroform, we observe an essentially fully averaged dipolar interaction. These observations accord overall with earlier reports on chloroform encaged in a larger host, cryptophane-E (with three

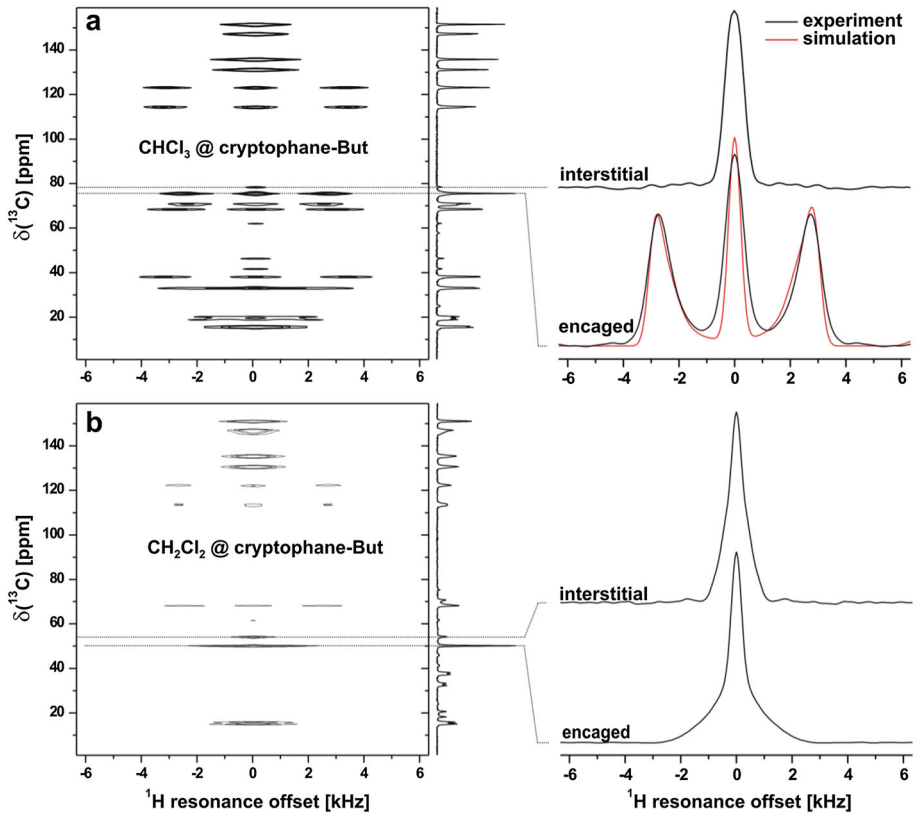

Figure 3. (Left panel) ^{13}C spectra recorded by the 2D separated local field NMR protocol from powders of (a) $CHCl_3$@cryptophane-But and (b) CH_2Cl_2@cryptophane-But. The 2D NMR spectra are presented such that the various ^{13}C resonances from host/guest molecules are resolved along the vertical (ν_2) spectral dimension, while its horizontal (ν_1) counterpart comprises information about the recoupled ^{1}H-^{13}C dipolar interactions. (right panel) Selected slices along the ν_1 dimension at the as-indicated ^{13}C sites, including each 'interstitial' and 'encaged' guest molecule. The red traces represent numerically simulated peak shapes used to extract the value of the motionally averaged dipolar interactions. The relatively intense centre peak of each recoupled peak shape is an undesirable feature of the experiment, but it does not compromise the dipolar coupling-estimates (see ref. 18 for further discussions). The lowest 2D contour level is set at about 5% of the maximum 2D peak amplitude in each spectrum.

linkers with $n = 3$), $|b_{C\text{-}H}| = 19.0$ kHz,[14] as well as with relaxation measurements in solution.[31–34] For the 'interstitial' (here perhaps adsorbed) site, the earlier study[14] displayed a sizable splitting not observed here. Indeed, the presence of the butoxy chains in the cryptophane makes the system to crystallize differently, thereby affecting the motions of the chloroform molecules.

Contrary to the case of chloroform, the 2D SLF NMR spectrum observed from CH_2Cl_2@cryptophane-But [Fig. 3(b)] manifests no dipolar splittings of guest molecules, with an estimated upper limit $|b_{C\text{–}H}| < 3$ kHz of the residual dipolar coupling that could pass undetected. The interstitial molecules gave a very similar result. This suggests that their motions are isotropic and thereby make the dipolar interaction to vanish. The same result was obtained from a 2D SLF experiment performed at a lower temperature of 203 K (not shown). We also note that significant recoupling effects are observed for the CH_2 aliphatic linkers of the cryptophane-But host (Fig. 3), evidencing a successful operation of the heteronuclear recoupling, as further illustrated for the 1″ $^{13}CH_2$ groups in each respective 2D NMR spectrum (Supporting information). We have previously observed low residual dipolar couplings of 3.3 kHz (in the solid state) and 3.2 ± 0.3 kHz (from NMR relaxation in solution) for dichloromethane encaged in cryptophane-E, with its fairly large cavity.[14] In the case of CH_2Cl_2@cryptophane-A, we measured the residual coupling of 14.2 ± 0.9 kHz, while intermediate values were reported for cryptophanes with linkers of mixed lengths ($n = 2$ and $n = 3$).[4] From that study, we concluded that the restricted mobility of the dichloromethane molecule in a cryptophane cavity becomes more confined when the size of the cavity is reduced. Neglecting the substituents on the phenyl groups, the cavity of cryptophane-But should be identical to that of cryptophane-A, except for perhaps a different distribution of the linker conformations (see succeeding dicussions). This might result in a somewhat larger cavity. In any case, the vanishing dipolar interaction of CH_2Cl_2 in cryptophane-But is unexpected.

Single crystal X-ray diffraction

In order to rationalize the unexpected finding of a vanishing ^{13}C-^{1}H interaction in the case of dichloromethane guest, we performed single crystal XRD experiments on the cryptophane-But complexes of chloroform and dichloromethane. Both systems crystallize in the trigonal space group *R*-3*c*. As expected, the cryptophane cages were found to be isostructural with substantial disorder present in the butoxy chains. As mentioned previously, the -O-$(CH_2)_2$-O- linkers are slightly disordered but the dominant conformation is *trans*. The orientation of the guest molecules within the cryptophane cavity is shown in Fig. 4. In both cases, the chlorine atoms are oriented towards the opening of the cavity, whereas the carbon atoms are located close to the −3 rotation axis.

For $CHCl_3$@cryptophane-But, the chloroform molecule was found to be disordered over four positions. For CH_2Cl_2@cryptophane-But, dichloromethane molecules occupy 12 distinct positions. The reason for the larger number of disordered positions for CH_2Cl_2 is its smaller size and the lack of a threefold rotation axis. The disorder of the guest molecules can also be observed from the electron density maps shown in the Supporting information. By superimposing the structural model, it is evident that the refined atom positions agree with what is observed from the electron density maps, while the electron density was insignificant in the rest of the cavity.

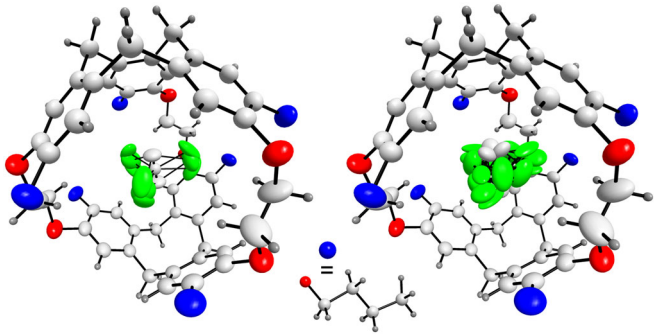

Figure 4. X-ray structures of $CHCl_3$@cryptophane-But (left) and CH_2Cl_2@cryptophane-But (right). The blue ellipsoids refer to the butoxy groups.

We could not identify any interstitially located guests, which can be explained either by structural disorder at these locations, or as a corroboration of the alternative interpretation of the NMR data in terms of chloromethanes adsorbed on the crystal surfaces. It is perhaps possible to interpret the XRD-derived structures as indicative of a slightly lower ordering of encaged dichloromethane guests compared with those of chloroform, but the XRD data as such cannot explain the vanishing residual dipolar coupling for the former system.

NMR relaxation in the liquid state

The XRD-derived structures provide a structural average but give no information on possible dynamic disorder, i.e. disorder because of molecular motions. On the other hand, the molecular motions can be sensitively probed by ^{13}C NMR relaxation measurements. In our recent solution NMR study of cryptophane-But complexes over a wide temperature range,[9] we found that the CH_2Cl_2@cryptophane-But system exhibited slow exchange (on the chemical shift time scale) of the guest between the encaged site and the free site in solution. However, the exchange was fast enough to have a strong effect on the spin-lattice relaxation measurements of the two sites, not investigated further in that study. We return to this issue here.

To probe the mobility of dichloromethane within the host cavity, the longitudinal relaxation of the free and the bound guest was investigated by using a series of 2D heteronuclear HSQC-type experiments.[26] The results are shown in Fig. 5. The results of Fig. 5 reveal that the spin-lattice relaxation curves for the free (left) and the bound (right) sites show a bi-exponential behaviour because of chemical exchange.[35] In order to determine the relaxation and the exchange rates, the time-dependence of the longitudinal magnetization has to be treated according to the Bloch–McConnell equations.[36–38] For a two-site chemically exchanging system, the evolution of the longitudinal magnetization for the free and the bound sites Mz_f and Mz_b can be expressed as[39]

$$\frac{dMz_f}{dt} = R_1^f\left(Mz_f^\infty - Mz_f\right) - k_{fb}Mz_f + k_{bf}Mz_b \quad (1)$$

$$\frac{dMz_b}{dt} = R_1^b\left(Mz_b^\infty - Mz_b\right) - k_{bf}Mz_b + k_{fb}Mz_f \quad (2)$$

where Mz_f^∞ and Mz_b^∞ correspond to the equilibrium magnetizations, R_1^f and R_1^b the respective longitudinal relaxation rates in the absence of exchange, while k_{fb} is the rate constant for the

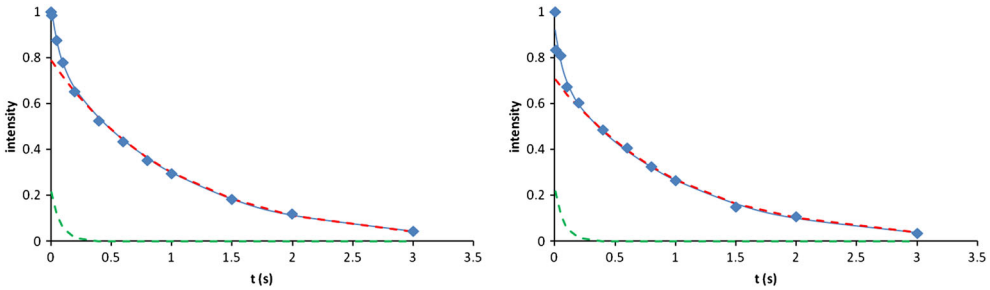

Figure 5. Result of the HSQC-type inversion-recovery experiments and the bi-exponential fitting for the free (left) and the bound (right) relaxation curves. The dashed lines represent the two exponentials.

transition from free to bound sites (with k_{bf} representing that of the reversed process). The solutions to these coupled equations are as follows:

$$Mz_f(t) = \Lambda_1 e^{\lambda_1 t} + \Lambda_2 e^{\lambda_2 t} + Mz_f^{\infty} \tag{3}$$

$$Mz_b(t) = \Lambda_3 e^{\lambda_1 t} + \Lambda_4 e^{\lambda_2 t} + Mz_b^{\infty} \tag{4}$$

with

$$\lambda_1 = 1/2\left[-\left(R_1^f + k_{fb} + R_1^b + k_{bf}\right) + \sqrt{\left(R_1^f + k_{fb} - R_1^b - k_{bf}\right)^2 + 4k_{fb}k_{bf}}\right] \tag{5}$$

and

$$\lambda_2 = 1/2\left[-\left(R_1^f + k_{fb} + R_1^b + k_{bf}\right) - \sqrt{\left(R_1^f + k_{fb} - R_1^b - k_{bf}\right)^2 + 4k_{fb}k_{bf}}\right] \tag{6}$$

Λ_1, Λ_2, Λ_3 and Λ_4 are the amplitudes of the exponentials; their expressions are given elsewhere.[39]

Before fitting the parameters of Eqns 3–6 to the experimental data, two assumptions are made: (1) the free site relaxation rate ($R_1{}^f = 0.17\ s^{-1}$) is fixed at the value obtained from an independent experiment on a dilute CH_2Cl_2 sample in the tetrachloroethane solvent without cryptophane. (2) The value of the ratio between the two exchange rates $k_{fb}/k_{bf} = p_b/p_f = 4.5$ is taken from our earlier work[9] at 245 K, where $p_b = 0.82$ and $p_f = 0.18$ are the relative populations of the bound and free site, respectively. The fitting of the T_1 relaxation curves was achieved by a nonlinear least-squares analysis using the Simplex algorithm and Matlab software.[40] The parameters R_1^b and k_{fb} were optimized. The errors on the optimized values were obtained from 500 Monte Carlo iterations by considering an error of 5% on the experimental data and an error of 20% on the assumed ratio k_{fb}/k_{bf}. The results are shown in Table 2 and in Fig. 5.

The two exponential decay rates, λ_1 and λ_2, given by Eqns (5) and (6) with the parameters from Table 2 are −1.0 and −15.0. The former number is very close to the population-averaged relaxation rate:[38]

$$R_1^{obs} = (1 - p_b)R_1^f + p_b R_1^b \tag{7}$$

while the latter is similar to the sum of the two exchange rates. Thus, we may conclude that the results conform to the limit of exchange being slow on the chemical shift time scale but much faster than relaxation.

From the relaxation results, we can obtain some information concerning the re-orientational dynamics of dichloromethane within the host cavity by using the Lipari–Szabo 'model-free' approach.[41] According to this model, the spectral density is

$$J(\omega) = \frac{2}{5}\left[\frac{S^2\tau_G}{1 + \omega^2\tau_G^2} + \frac{(1 - S^2)\tau_{\text{eff}}}{1 + \omega^2\tau_{\text{eff}}^2}\right] \tag{8}$$

with

$$\tau_{\text{eff}}^{-1} = \tau_G^{-1} + \tau_{\text{loc}}^{-1} \tag{9}$$

where τ_G is a rotational correlation time characterizing the isotropic global rotational diffusion, τ_{loc} is a local correlation time, and S^2 is the generalized order parameter squared describing the spatial restrictions of the internal motions.

From the NMR solid-state experiments, we found that the motion of dichloromethane within the cryptophane-But cavity is completely unrestricted, i.e. isotropic. This result leads then to $S^2 = 0$ so that the spectral density becomes

$$J(\omega) = \frac{2}{5}\left[\frac{\tau_{\text{eff}}}{1 + \omega^2\tau_{\text{eff}}^2}\right] \tag{10}$$

Considering the expression of the relaxation rate in the case of dominant dipolar interactions,[33]

$$R_1 = \frac{1}{4}N_H b_{CH}{}^2[J(\omega_H - \omega_C) + 3J(\omega_C) + 6J(\omega_H + \omega_C)] \tag{11}$$

with $N_H = 2$ being the number of protons attached to the ^{13}C nucleus and

$$b_{CH} = -\frac{\mu_0\gamma_H\gamma_C\hbar}{4\pi r_{CH}{}^3} \tag{12}$$

the dipole–dipole coupling constant. Assuming that $r_{CH} = 107.3$ pm and using the previously derived value of R_1^b found in the previous discussions, the correlation time associated with the motion of the bound CH_2Cl_2 within the cavity is estimated to be around 30 ps, which is in reasonable agreement with the values found earlier for the same guest in other cryptophane cavities.[4] This result from solution-state NMR is thus consistent with that obtained in the solid state.

Table 2. Optimized parameters from the fitting of the T_1 relaxation curves

	Relaxation rates (s^{-1})	Exchange rates (s^{-1})
Free site	$R_1^f = 0.17$	$k_{fb} = 12 \pm 5$
Bound site	$R_1^b = 1.2 \pm 0.2$	$k_{bf} = 2.6 \pm 1.1$

Concluding remarks

Estimated residual dipolar ^{13}C-^{1}H interactions for chloroform and dichloromethane encaged within cryptophane-But cavity by solid-state 2D SLF ^{13}C NMR revealed a relatively large dipolar coupling constant ($b|_{C\text{-}H}| = 19.0$ kHz) in the case of chloroform guest, while the dipole–dipole interaction for dichloromethane guest were fully averaged out. Noteworthy, the present 2D SLF experimentation involved a significantly lower ^{13}C isotopic enrichment than those utilized in our previous cryptophane studies: The present experiments are readily performed at a natural abundance level of ^{13}C at a modest field of 9.4 T, as may be appreciated from the sufficient NMR data quality of all ^{13}C signals from cryptophane-But in Fig. 3. Although not targeted in the present study, all sets of heteronuclear contacts of the host molecules are readily extracted from the 2D spectra.

Because the solid-state NMR result for the dichloromethane guest is unexpected, we utilized single crystal XRD to unambiguously confirm the occurrence of the dichloromethane guests within the cryptophane-But cavity. Moreover, XRD revealed the presence of static or dynamic disorder of the encaged guests. To further characterize the CH_2Cl_2 dynamics inside the host, we reported a ^{13}C relaxation study in the solution. The system is characterized by exchange rates between free and encaged guest molecules that are slow on the chemical shift time scale but fast compared with the ^{13}C spin-lattice relaxation. This complicates the analysis of the detailed guest dynamics. Nevertheless, we found that the solution-state relaxation data are consistent with a fast and isotropic reorientation of the CH_2Cl_2 molecule within the cryptophane-But cavity.

Acknowledgements

This work was supported by the Swedish Research Council (Grant No. 613-2011-3311) and the Carl Tryggers Foundation. The financial support of the Swedish Research Council and the Knut and Alice Wallenberg Foundation allowing purchase of the solid state NMR equipment is gratefully acknowledged. We would like to thank Mr Torbjörn Astlind for his help with the liquid-state NMR spectrometer.

References

[1] J. Gabard, A. Collet. *J. Chem. Soc. Chem. Comm.* **1981**, 1137–1139. DOI:10.1039/C39810001137.
[2] A. Collet, J. Gabard, J. Jacques, M. Cesario, J. Guilhem, C. Pascard. *J. Chem. Soc. Perkin Trans. I.* **1981**, 1630–1638. DOI:10.1039/P19810001630.
[3] D. Cavagnat, T. Brotin, J. L. Bruneel, J. P. Dutasta, A. Thozet, M. Perrin, F. Guillaume. *J. Phys. Chem. B* **2004**, *108*, 5572–5581. DOI:10.1021/jp0375158.
[4] S. Nikkhou Aski, A. Y. H. Lo, T. Brotin, J. P. Dutasta, M. Edén, J. Kowalewski. *J. Phys. Chem. C* **2008**, *112*, 13873–13881. DOI:10.1021/jp8039498.
[5] T. Brotin, T. Devic, A. Lesage, L. Emsley, A. Collet. *Chem. Eur. J.* **2001**, *7*, 1561–1573. DOI:10.1002/1521-3765(20010401)7:7<1561::AID-CHEM1561>3.0.CO;2-9.
[6] T. Brotin, J. P. Dutasta. *Chem. Rev.* **2009**, *109*, 88–130. DOI:10.1021/cr0680437.
[7] T. Brotin, V. Roy, J. P. Dutasta. *J. Org. Chem.* **2005**, *70*, 6187–6195. DOI:10.1021/jo050495g.
[8] G. Huber, L. Beguin, H. Desvaux, T. Brotin, H. A. Fogarty, J. P. Dutasta, P. Berthault. *J. Phys. Chem. A* **2008**, *112*, 11363–11372. DOI:10.1021/jp807425t.
[9] Z. Takacs, E. Steiner, J. Kowalewski, T. Brotin. *J. Phys. Chem. B* **2014**, *118*, 2134–2146. DOI:10.1021/jp4105272.
[10] J. Canceill, M. Cesario, A. Collet, J. Guilhem, C. Pascard. *J. Chem. Soc. Chem. Comm.* **1985**, 361–363. DOI:10.1039/C39850000361.
[11] J. Canceill, M. Cesario, A. Collet, J. Guilhem, L. Lacombe, B. Lozach, C. Pascard. *Angew. Chem. Int. Ed.* **1989**, *28*, 1246–1248. DOI:10.1002/anie.198912461.
[12] O. Petrov, Z. Tosner, I. Csöregh, J. Kowalewski, D. Sandström. *J. Phys. Chem. A* **2005**, *109*, 4442–4451. DOI:10.1021/jp044884a.
[13] O. Taratula, P. A. Hill, N. S. Khan, P. J. Carroll, I. J. Dmochowski. *Nat. Commun.* **2010**, *1*, 148. DOI:10.1038/ncomms1151.
[14] Z. Tosner, O. Petrov, S. V. Dvinskikh, J. Kowalewski, D. Sandström. *Chem. Phys. Lett.* **2004**, *388*, 208–211. DOI:10.1016/j.cplett.2004.02.091.
[15] M. G. Munowitz, R. G. Griffin, G. Bodenhausen, T. H. Huang. *J. Am. Chem. Soc.* **1981**, *103*, 2529–2533. DOI:10.1021/ja00400a007.
[16] G. Metz, X. Wu, S. O. Smith. *J. Magn. Reson. Ser. A* **1994**, *110*, 219–227. DOI:10.1006/jmra.1994.1208.
[17] A. E. Bennett, C. M. Rienstra, M. Auger, K. V. Lakshmi, R. G. Griffin. *J. Chem. Phys.* **1995**, *103*, 6951–6958. DOI:10.1063/1.470372.
[18] X. Zhao, M. Edén, M. H. Levitt. *Chem. Phys. Lett.* **2001**, *342*, 353–361. DOI:10.1016/S0009-2614(01)00593-0.
[19] M. Carravetta, M. Edén, X. Zhao, A. Brinkmann, M. H. Levitt. *Chem. Phys. Lett.* **2000**, *321*, 205–215. DOI:10.1016/S0009-2614(00)00340-7.
[20] Oxford diffraction, *CrysAlisCCD and CrysAlisRED*, Oxford diffraction LtD, Abingdon, Oxfordshire, England, **2006**.
[21] A. Altomare, G. Cascarano, C. Giacovazzo, A. Guagliardi, M. C. Burla, G. Ploidori, M. Camalli. *J. Appl. Crystallogr.* **1994**, *27*, 435–436. DOI:10.1107/S002188989400021X.
[22] G. M. Sheldrick. *Acta Crystallogr. A: Found. Crystallogr.* **2008**, *64*, 112–122. DOI:10.1107/S0108767307043930.
[23] L. J. Farrugia. *J. Appl. Crystallogr.* **1999**, *32*, 837–838. DOI:10.1107/S0021889899006020.
[24] G. Bergerhoff, *DIAMOND*, Crystal Impact GbR, Bonn, Germany, **1996**.
[25] K. Momma, F. Izumi. *J. Appl. Crystallogr.* **2011**, *44*, 1272–1276. DOI:10.1107/S0021889811038970.
[26] I. Bertini, M. M. J. Couture, A. Donaire, L. D. Eltis, I. C. Felli, C. Luchinat, M. Piccioli, A. Rosato. *Eur. J. Biochem.* **1996**, *241*, 440–452. DOI:10.1111/j.1432-1033.1996.00440.x.
[27] G. Bodenhausen, D. J. Ruben. *Chem. Phys. Lett.* **1980**, *69*, 185–189. DOI:10.1016/0009-2614(80)80041-8.
[28] A. G. Palmer III, J. Cavanagh, P. E. Wright, M. Rance. *J. Magn. Reson.* **1991**, *93*, 151–170. DOI:10.1016/0022-2364(91)90036-S.
[29] G. Kontaxis, J. Stonehouse, E. D. Laue, J. Keeler. *J. Magn. Reson. A* **1994**, *111*, 70–76. DOI:10.1006/jmra.1994.1227.
[30] S. N. Ghosh, R. Trambarulo, W. Gordy. *J. Chem. Phys.* **1952**, *20*, 605–607. DOI:10.1063/1.1700501.
[31] J. Lang, J. J. Dechter, M. Effemey, J. Kowalewski. *J. Am. Chem. Soc.* **2001**, *123*, 7852–7858. DOI:10.1021/ja004349y.
[32] Z. Takacs, M. Soltesova, D. Kotsyubynskyy, J. Kowalewski, J. Lang, T. Brotin, J. P. Dutasta. *Magn. Reson. Chem.* **2010**, *48*, 623–629. DOI:10.1002/mrc.2637.
[33] Z. Takacs, M. Soltesova, J. Kowalewski, J. Lang, T. Brotin, J. P. Dutasta. *Magn. Reson. Chem.* **2013**, *51*, 19–31. DOI:10.1002/mrc.3898.
[34] Z. Takacs, T. Brotin, J. P. Dutasta, J. Lang, G. Todde, J. Kowalewski. *J. Phys. Chem. B* **2012**, *116*, 7898–7913. DOI:10.1021/jp303469x.
[35] A. D. Bain. *Prog. Nucl. Magn. Reson. Spectrosc.* **2003**, *43*, 63–103. DOI:10.1016/j.pnmrs.2003.08.001.
[36] H. M. McConnell. *J. Chem. Phys.* **1958**, *28*, 430–431. DOI:10.1063/1.1744152.
[37] J. S. Leigh Jr.. *J. Magn. Reson.* **1971**, *4*, 308–311. DOI:10.1016/0022-2364(71)90040-0.
[38] J. Kowalewski, L. Mäler, *Nuclear Spin Relaxation in Liquids*, Taylor and Francis, New York, **2006**.
[39] D. Flemming Hansen, J. J. Led. *J. Magn. Reson.* **2003**, *163*, 215–227. DOI:10.1016/S1090-7807(03)00062-4.
[40] D. C. Hanselman, B. R. Littlefield, *Mastering Matlab 6: A Comprehensive Tutorial and Reference*, Prentice Hall, Upper Saddle River, NJ, **2001**.
[41] G. Lipari, A. Szabo. *J. Am. Chem. Soc.* **1982**, *104*, 4546–4559. DOI:10.1021/ja00381a009.

Supporting Information

Additional supporting information may be found in the online version of this article at the publisher's web site.